Highlights

►Carbonylation protein profiles were evaluated in high-fat high-sucrose-fed rats. ►High-fat high-sucrose diet increased plasma and liver global protein carbonylation. ►HFHS diet triggers carbonylation of several specific proteins that were identified. ►Specific protein carbonylation seems related to hyperinsulinemia, NAFLD and obesity.

PROTEIN CARBONYLATION ASSOCIATED TO HIGH-FAT HIGH-SUCROSE DIET AND ITS METABOLIC EFFECTS

Lucía Méndez[1]*, Manuel Pazos[1], Eunice Molinar–Toribio[2], Vanesa Sánchez–Martos[3], José M. Gallardo[1], M. Rosa Nogués[3], Josep L. Torres[2] and Isabel Medina[1]

[1]Instituto de Investigaciones Marinas, Consejo Superior de Investigaciones Científicas (IIM–CSIC), E–36208 Vigo, Spain.

[2]Instituto de Química Avanzada de Catalunya, Consejo Superior de Investigaciones Científicas (IQAC–CSIC), E–08034 Barcelona, Spain

[3]Unidad de Farmacología. Facultad de Medicina y Ciencias de la Salud, Universidad Rovira i Virgili, E–43201 Reus, Spain

*Author to whom correspondence should be addressed [e–mail: luciamendez@iim.csic.es; telephone +34 986 231930; fax +34 986 292762].

Running title: Redox proteomics on high–fat high–sucrose diets

Abstract

The present research draws a map of the characteristic carbonylation of proteins in rats fed high caloric diets with the aim of providing a new insight of the pathogenesis of metabolic diseases derived from the high consumption of fat and refined carbohydrates. Protein carbonylation was analyzed in plasma, liver and skeletal muscle of Sprague–Dawley rats fed a high–fat high–sucrose (HFHS) diet by a proteomics approach based on carbonyl–specific fluorescence–labelling, gel electrophoresis and mass spectrometry. Oxidized proteins along with specific sites of oxidative damage were identified and discussed to illustrate the consequences of protein oxidation. The results indicated that long–term HFHS consumption increased protein oxidation in plasma and liver, meanwhile protein carbonyls from skeletal muscle did not change. The increment of carbonylation by HFHS diet was singularly selective on specific target proteins: albumin from plasma and liver, and hepatic proteins such as mitochondrial carbamoyl–phosphate synthase (ammonia), mitochondrial aldehyde dehydrogenase, argininosuccinate synthetase, regucalcin, mitochondrial ATP synthase subunit beta, actin cytoplasmic 1, mitochondrial glutamate dehydrogenase 1. The possible consequences that these specific protein carbonylations have on the excessive weight gain, insulin resistance and nonalcoholic fatty liver disease resulting from HFHS diet consumption have been discussed.

Keywords: High–fat high–sucrose diet; Obesity; Insulin resistance; NAFLD, Protein carbonylation; Sprague–Dawley rat

1. Introduction

Protein carbonylation constitutes the most common biomarker of oxidative protein damage and can be induced by the attack of reactive oxygen species (ROS) [1]. The consumption of high caloric diets associated to westernized life style has been linked to the generation of an excess of ROS, particularly superoxide anion through the mitochondrial electron–transport chain, and to the development of multiple metabolic disorders as obesity, hypertension, hyperglycemia, hyperinsulinemia or dyslipidemia [2–4]. As consequence of this ROS overproduction, increased protein carbonylation levels have been described occurring together with these diet–induced disorders [5, 6].

Protein carbonylation is an irreversible oxidative post–translational modification, although cells exhibit native enzymatic systems that eliminate altered proteins and maintain cellular homeostasis and survival. These damage response systems are typically proteasome in the cytosol and ATP–dependent proteases in mitochondria [7]. When these enzymatic systems come to fail, carbonylated proteins accumulate in the cell and cellular functions disrupt because carbonylated proteins either lose their catalytic and structural integrity, or interrupt regulatory pathways [8].

Protein oxidative damage has been traditionally accepted to be a random process since ROS generally attack protein non–enzymatically and radical species such as hydroxyl radicals are so reactive that are able to oxidize most amino acids [9]. However, several studies have revealed that protein carbonylation is highly selective in diseases as Alzheimer [10] or uremia [11], or even during the natural aging process. A dietary intervention study of Wistar rats supplemented with fish oils also showed such specificity by down–regulating carbonylation of several plasma and liver proteins [12]. However, to date few studies have addressed protein oxidation linked to metabolic disorders induced by diet high in fat and/or sugars, and those that exist performed essentially total protein carbonylation measurements [13–17].

The aim of the present study is to evaluate comprehensively the impact of oxidative stress triggered by HFHS diets on irreversible oxidative protein damage, and particularly, on protein carbonylation. Recent investigations indicated that obesity and insulin resistance are accompanied by an increase carbonylation of certain adipose–regulatory proteins [6, 18]. The present work is focused on the explicit carbonylation of plasma, liver and skeletal muscle proteins since these tissues play a key role in the development of metabolic disorders [19], and they have not been addressed before. To this purpose, we analyzed total and individual protein carbonylation in plasma, liver and skeletal muscle from rats fed a HFHS diet for 22 weeks, compared with control rats fed a low–fat diet. Proteins susceptible to oxidation and carbonylation sites were identified by using a proteomics approach based on gel electrophoresis and protein identification by tandem mass spectrometry (MS/MS). Protein carbonylation was correlated with morphological measurements, and biochemical parameters of lipid and carbohydrate metabolism, lipid peroxidation products and endogenous antioxidant systems, and discussed in terms of its potential implication on the metabolic disorders observed.

2. Materials and methods

2.1. Materials and reagents

Fluorescein–5–thiosemicarbazide (FTSC) was purchased from Invitrogen (Carlsbad, CA, USA) and porcine sequencing grade modified trypsin was from Promega (Madison, WI, USA). Ketamine chlorhydrate (Imalgene 1000) was purchased from Merial Laboratorios S.A. (Barcelona, Spain) and xylacine (Rompun 2%) was from Quimica Farmaceutica S.A. (Barcelona, Spain). ProteoBlock™ protease inhibitor cocktail was purchased from Thermo Fisher Scientific Inc. (Rockford, IL, USA). Phenylmethylsulfonyl fluoride (PMSF), dithiothreitol (DTT), iodoacetamide, ethylenediaminetetraacetic acid (EDTA), trichloroacetic acid (TCA), Tris–HCl, 3,3–cholaminopropyl–dimethylammonio–1–propanesulfonate (CHAPS), sodium phosphate, magnesium chloride anhydrous, AAPH (2,2´–azobis(2–amidinopropane) dihydrochloride), fluorescein (3´,6´–dihydroxyspiro[isobenzofuran–1[3H],9´[9H]–xanthen]–3–one), Trolox (6–hydroxy–2,5,7,8–tetramethylchroman–2–carboxylic acid), 2–thiobarbituric acid, 1,1,3,3,–tetraethoxypropane, propyl gallate and bicinchoninic acid (BCA) were purchased from Sigma–Aldrich (St. Louis, MO, USA). Urea, thiourea, sodium dodecyl sulfate (SDS), glycine, glycerol and Serdolit MB–1 were obtained from USB (Cleveland, OH, USA). IPG buffer, pharmalyte 3–10, ammonium persulfate (APS), bromophenol blue, 1,2–bis(dimethylamino)ethane (TEMED) were purchased from GE Healthcare Science (Uppsala, Sweden). Acrylamide, bis–*N,N´*–methylene–bis–acrylamide and Bio–Rad protein assay were obtained from Bio–rad (Hercules, CA, USA). All other chemicals and reagents used were of analytical reagent grade and water was purified using a Milli–Q system (Millipore, Billerica, MA, USA).

2.2. Animals and experimental design

Male 22–week–old Sprague–Dawley rats weighing between 500–600 g (Janvier, Le Genest–St–Isle, France) were housed in animal cages (*n* 2–3/cage) with a constantly regulated temperature (22 ± 2 °C), humidity (50 ± 10%) and light–controlled room (lights on 0630–1830). The animals were randomly assigned to one of two dietary groups: a control group (n=5) fed the reference diet Teklad Global 2014 (Harlan Teklad Inc., Indianapolis, IN, USA) and a group (n=5) fed a high–fat high–sucrose diet (HFHS) based on TD. 08811 diet (Harlan Teklad Inc). Rats had *ad libitum* access to water and food. Food intake and water consumption were registered daily throughout the study (means are showed in Table 1). After 22 weeks of experiment, rats were fasted overnight, anesthetized intraperitoneally with ketamine and xylacine (80 mg/kg and 10 mg/kg body weight respectively), and then killed by exsanguination. The control diet composition was (% by weight): 4.3% fat (3.9% soybean oil), 46.7% available carbohydrate (41% corn and wheat starches), 16.3% protein, 21.5 % total fiber, 4.6% minerals and 1.2% vitamins. Fats provided 13.3% of calories, carbohydrates provided 64.3% and proteins 22.5%. Total energy density was 2.9 Kcal/g. HFHS diet composition was (% by weight): 24.3% fat (21% anhydrous milkfat, 2% soybean oil), 43.5% available carbohydrate (32.4% sucrose), 20.9% protein, 4.7 % total fiber (from cellulose), 4.1% minerals, 1.8% vitamins (from AIN–93–VX (94047)) and 0.004% antioxidants. Fats provided 45.9% of calories, carbohydrates provided 36.5% (27% from sucrose) and proteins 17.6%. Total energy density was 4.7 Kcal/g. The approximate fatty acid profile of control diet (% of total fat) was: 18% saturated fatty acids (SFA), 20% monounsaturated fatty acids (MFA) and 62% polyunsaturated fatty acids (PUFA). In the HFHS diet, the fatty acid profile was: 61% SFA, 31% MUFA, and 8% PUFA. HFHS diet contained about 0.05% of cholesterol, mainly from the anhydrous milkfat. Control diet can contain small amounts of cholesterol, likely minor 0.001%. All the procedures followed the

European Union guidelines for the care and management of laboratory animals and all efforts were made to minimize suffering. The pertinent permission for this specific study was obtained from the CSIC (Spanish Research Council) Subcommittee of Bioethical Issues (ref. AGL2009–12 374–C03–03).

2.3. Sample collection

Total abdominal fat, corresponding to the sum of epididymal, perirenal and mesenteric depots, liver and skeletal muscle from hind leg were excised, washed with 0.9% NaCl solution, weighed and immediately frozen in liquid nitrogen upon sacrifice. The adiposity index ((total abdominal fat × 100)/body weight) and hepatosomatic index ((liver weight × 100)/body weight) were determined. One part of dissected livers was used for histological analysis. Blood samples were collected on a tube with EDTA by cardiac puncture, and plasma and erythrocyte samples were separated by centrifugation (850 g, 4ºC, 15 min.). Plasma samples for protein oxidation measurement were supplemented with 5 mM PMSF. All samples were stored at −80 ºC until analysis.

2.4. Biochemical measurements

Triglycerides, cholesterol, LDL cholesterol and HDL cholesterol were measured by spectrophotometric methods (SpinReact Kits, Girona, Spain) [20, 21]. The percentage of glycated hemoglobin, or HbA1c, in the blood was determined according to Sharp et al. [22]. Blood glucose levels were measured by an enzyme electrode method using the Ascensia ELITE

XL blood glucose meter (Bayer Consumer Care AG, Basel, Switzerland). Plasma insulin concentrations were measured using a Rat/Mouse Insulin ELISA kit according to the manufacturer's instructions (Millipore Corporation, Billerica, MA, USA).

2.5. Determination of lipid peroxidation levels and antioxidant systems in blood and liver samples

For estimating lipid peroxidation levels, we measured three different products of lipid peroxidation: lipid hydroperoxides (primary lipid oxidation product), conjugated dienes (intermediate oxidation product) and malondialdehyde (end oxidation product). The first step for the estimation of lipid hydroperoxides and conjugated dienes was to extract liver lipids with dichloromethane [23] and to determine total lipid content [24]. Then, conjugated dienes were measured following the AOCS method [25], and lipid hydroperoxides following the method of Chapman and Mackay [26]. We also measured total malondialdehyde (MDA) concentrations in plasma and liver. Total MDA was derivatized with thiobarbituric acid (TBA) after protein hydrolysis [27] and precipitation [28], and determined by HPLC–fluorescence according to Fukunaga et al. [29]. Total superoxide dismutase (SOD) activity was measured in plasma and liver following the method of Misra and Fridovich [30]. Catalase (CAT) activity was measured in plasma and liver according to the procedure of Cohen et al. [31]. Glutathione peroxidase (Gpx) and glutathione reductase (GR) activities were determined according to Wheeler et al. [32]. The oxidized and reduced glutathione balance (GSSG/GSH) was measured by the Hissin and Hilf fluorometric method [33]. The oxygen radical absorbance capacity (ORAC) from plasma and liver was determined according to Ou et al. [34]. ORAC measures antioxidant scavenging activity against peroxyl radicals induced by AAPH, using fluorescein as fluorescent probe and Trolox as standard and quality control.

2.6. Liver histological studies

Livers fixed in formalin were dehydrated in alcohol and embedded in paraffin. Serial liver sections (3 µm) were stained with haematoxylin/eosin (Harris Hematoxylin, Química Clínica Aplicada, S.A., Tarragona, Spain). Liver injury such as steatosis, lobular inflammation and fibrosis was evaluated by histological examination under a light microscope, as previously described [35]. Briefly, ten 200× light microscopic fields were viewed on each section and scored for the severity of hepatic steatosis, inflammation and fibrosis according to the following criteria: for hepatic steatosis (expressed as per cent of hepatocytes containing fat droplets): grade 0, no fat; grade 1, steatosis occupying less than 33% of the hepatic parenchyma; grade 2, 34–66% of the hepatic parenchyma; grade 3, more than 66% of the hepatic parenchyma; for inflammatory cell infiltration (graded on the basis of the presence of inflammatory cells): grade 0: none; grade 1, 1–2 foci/field; grade 2, 3–4 foci/field; grade 3, more than 4 foci/field. The staging of hepatic fibrosis was investigated as follows: 0, none; 1, mild, zone 3, perisinusoidal; 2, moderate, zone 3, perisinusoidal; 3, portal/periportal; 4, bridging fibrosis.

2.7. Protein extraction and fractionation

To reduce sample complexity, proteins from liver and skeletal muscle were fractioned according to hydrophobicity, into proteins soluble at low ionic strength (LIS fraction), mostly water–soluble proteins, and proteins soluble at high ionic strength (HIS fraction), mostly containing hydrophobic proteins associated with the various membranes in the cell. This sample fractionation improves sensitivity of water–soluble low abundance proteins. Between 200–400 mg of either liver or muscle were homogenized with an Ultra–Turrax high–performance disperser, in 25 volumes of 20 mM sodium phosphate, pH 6.0, 0.5 mM $MgCl_2$, 1 mM EDTA and **10 μL/mL buffer of ProteoBlock**^{TM} **protease inhibitor cocktail (100 mM AEBSF HCl, 80 μM** aprotinin, 5 mM bestatin, 1.5 mM E64, 2 mM leupeptin and 1 mM pepstatin A). Homogenized samples were centrifuged at 100000 g for 1 h at 4 ºC, and LIS fraction was recovered in the supernatants. HIS fraction was isolated by homogenization of the remaining pellets in 10 volumes of 10 mM Tris–HCl, pH 7.2, 0.6 M NaCl, 1 mM EDTA and **10 μL/mL buffer of** ProteoBlock^{TM} protease inhibitor cocktail. After centrifugation at 16000 g for 15 min at 4 ºC, HIS fractions were contained in the supernatants. Protein concentration in each fraction was measured by the Bicinchoninic Acid (BCA) assay [36].

2.8. FTSC–labelling of protein carbonyls

Protein oxidation levels in plasma, liver and skeletal muscle were measured by a fluorescence–based assay as previously described [12, 37, 38]. Briefly, LIS or HIS protein fractions from liver, muscle and plasma samples were independently incubated with 1 mM fluorescein–5–thiosemicarbazide (FTSC) in the dark (37 ºC, 2.5 h). FTSC specifically labels protein carbonyls. Afterward, proteins were precipitated with an equal volume of 20% chilled TCA (w/v) and centrifuged at 16000 g (20 ºC, 10 min). The pellets were washed five times with 100% ethanol/ethyl acetate (1:1) to remove the FTSC excess, and finally re–dissolved in urea buffer (7 M urea, 2 M thiourea, 2% CHAPS, 0.5% Pharmalyte 3–10, 0.5% IPG 3–10 buffer and 0.4% DTT). FTSC–labelled proteins were stored at –80ºC until use. Protein concentration was determined by Bradford assay [39].

2.9. Gel electrophoresis–based evaluation of global and specific protein carbonylation levels

2.9.1. Gel electrophoresis and image analysis

To evaluate the effect of HFHS diets on protein carbonylation level, we used a proteomics approach based on gel electrophoresis. [40]. In order to analyze global protein carbonylation, 30 μg of each FTSC–labeled sample were subjected to 1–D (mono–dimensional) SDS–PAGE (sodium dodecyl sulfate–polyacrylamide gel electrophoresis), and run in a Mini–PROTEAN 3 cell (Bio–rad, Hercules, CA, USA). The analysis of carbonyl levels in specific proteins was performed by resolving FTSC–labelled proteins in 2–D electrophoresis gel [12, 38]. Briefly, 400 μg of protein were separated in 11–cm, pH 3–10, IPG strips (Immobiline™DryStrip gels, GE Healthcare Science, Uppsala, Sweden) by using an EttanIPGphor II isolectric focusing system (GE Healthcare Science) set at 20 ºC. After focusing, the strips were kept frozen at –80ºC until use. The second dimension was performed in laboratory–made 10% SDS–polyacrylamide gels by using an Ettan Daltsix electrophoresis system (GE Healthcare Science) at 15 ºC. Two 11–cm IPG strips corresponding to both diets were run in the same 2–D electrophoresis gel (24–cm wide) and 5 gels were running in each assay.

FTSC–tagged proteins were visualized by exposing 1–D or 2–D gels to a UV transilluminator Molecular Imager Gel Doc XR System (Bio–Rad, Hercules, CA, USA) equipped with a 520–nm band–pass filter (520DF30 62 mm). Then, gels were stained overnight with Coomassie dye PhastGel Blue R–350 (GE Healthcare Science) to visualize total protein level.

Image analysis of 1–D gels was performed with the 1–D gel analysis software LabImage 1D (Kapelan Bio–Imaging Solutions, Halle, Germany) on the basis of the overall optical volume per lane. Meanwhile, protein spots were detected and matched among 2–D gels by using the PDQuest software version 7.1 (Bio–Rad, Hercules). The intensity of the spots was expressed as parts per million (ppm) of the total integrated optical density of the gel, which was approximately constant among gels.

2.9.2. Calculation of carbonylation indexes

To analyze the influence of diet on protein carbonylation level, we calculated a concentration–normalized **"protein carbonylation index"** as previously described [12, 38], and compared that value between diets. This normalized parameter of carbonylation divides the fluorescence intensity of lane/band/spot in the FTSC–stained gel by the protein concentration represented by the intensity of Coomassie. Therefore, carbonylation index allows normalizing the protein carbonylation level (measured by FTSC–intensity in gel) with protein abundance (measured by Coomassie–intensity in gel) and offsetting possible differences in protein loading and protein concentration.

2.10. Identification of proteins by LC–ESI–IT–MS/MS

Spots corresponding to proteins of interest were excised from gels and digested *in situ* with sequencing grade bovine trypsin according to a protocol previously described [41]. Protein identity was ascertained by a LC system model SpectraSystem P4000 (Thermo Scientific, San Jose, CA, USA) coupled to an ion trap (IT) mass spectrometer model LCQ Deca XP Plus or LTQ Velos Pro with electrospray ionization (ESI) interface (Thermo Scientific). Tryptic peptides were separated on a BioBasic–18 RP column, 0.18 mm × 150 mm, 5 μm (Thermo Scientific) using 0.5% aqueous acetic acid and in 80% acetonitrile as mobile phases A and B, respectively. A 90 min linear gradient from 5 to 60% B, at a flow rate of 1.5–1.7 μL/min, was used. Peptides were detected using survey scans from 350 to 1600 Da (2 μscans), followed by MS/MS scans (2 μscans) of the six more intense peaks using an isolation width of 1 Da and a normalized collision energy of 35%. Fragmented masses were set in dynamic exclusion for 30 s after the second fragmentation event and singly charged ions were excluded from MS/MS analysis.

Protein identification was performed by homology of experimental MS/MS peak lists with theoretical MS/MS spectra contained in the *Rattus norvegicus* UniProtKB/Swiss–Prot database (28855 sequences) released in October 2013 by using the Sequest HT search engine (Proteome Discoverer 1.4., Thermo Scientific, San Jose, CA, USA). The following search criteria were applied: tryptic cleavage, up to 2 missed cleavage sites, and tolerances ±1.5 Da for precursor ions and ±0.8 Da for MS/MS fragment ions. Methionine oxidation and carbamidomethylation of cysteine were set as variable modifications. Also, up to 18 different carbonyl modifications of amino acids were searched as variable modifications. These carbonyl modifications resulted from the direct oxidation of side chains of amino acid residues (oxidation of histidine to 2–oxohistidine, oxidation of cysteine or serine to 3–oxoalanine, oxidation of threonine to 2–amino–

3–ketobutiric, oxidation of proline to glutamic semialdehyde or 5–oxoproline, oxidation of arginine to glutamic semialdehyde and oxidation of tryptophan to 3–hydroxykynurenine, kynurenine, N–fomylkynurenine, hydroxy–N–fomylkynurenine) or the adduction with carbonyls derived from lipid peroxidation and glycoxidation by Michael and/or Schiff base addition (MDA, acrolein, crotonaldehyde, 4–ONE, 2–hexenal, glyoxal, HNE, HHE, acetaldehyde). Since Sequest HT has the limitation of allowing just six modifications per search, several consecutive searches for each sample were required to explore oxidative sites of carbonyl modifications (Table 3 and supplementary Tables S1 and S2). MS/MS spectra were manually inspected to identify an oxidation site and confirm the amino acid. The FDR (false discovery rate) was kept below 1%.

2.11. Statistical analysis

Single biological replicates for each dietary treatment, control (n=5) and HFHS (n=5), were subjected to three independent experiments of FTSC carbonyl–labelling and gel electrophoresis. Therefore, 1–D and 2–D gels were performed at least three times for each type of protein fraction (LIS and HIS proteins) and biological sample (plasma, liver and skeletal muscle). Individual and global oxidation protein levels were reported as mean and standard deviation (SD). Statistical analysis was preformed using the Student *t* test with Statistica 6.0 program (Statsoft, Inc., Tulsa, OK, USA). The level of significant difference was set at $p < 0.05$.

3. Results

3.1. Metabolic changes induced by HFHS diet

No rat died in any group during the whole experimental period. The energy intake of HFHS rats was higher than controls throughout the experiment, rising to be approximately 24% higher since the ninth week, despite their lower food intake compared to controls (Table 1). This fact is explained by the much higher energy density of HFHS diet (4.7 Kcal/g) in comparison to the control diet (2.9 Kcal/g). HFHS group significantly increased body, abdominal and liver fat weights. Thus, at the end of experimental period, HFHS rats weighed almost 28% more than control rats and showed about 52% more abdominal fat. Accordingly, rats fed HFHS exhibited an adiposity index significantly higher (34%) than control rats. Livers of HFHS rats accumulated also 3.8-fold more lipids than rats fed a control diet. Although not statistically significant, the hepatosomatic index of HFHS rats also tended to increase (Table 1). Additionally, HFHS diet showed a significant effect on plasma insulin levels. Insulin concentrations were higher in rats fed HFHS diet than in control rats, and differences were significant from the fifth week on. Other parameters as plasma glucose, HbA1c percentage, total cholesterol, LDL and HDL cholesterol and triglycerides did not change significantly between diets.

Histological features of the liver revealed hepatic steatosis and lobular inflammation in the group of HFHS animals (Figure 1B, 1C and 1D). In contrast, rats fed control diet did not show a significant fat accumulation and inflammation in liver (Figure 1A). No liver showed fibrosis.

In regards to the parameters associated to oxidative stress, Table 2 shows the level of lipid peroxidation, antioxidant enzyme activity and antioxidant capacity in plasma and liver. HFHS livers showed higher lipid peroxidation in terms of lipid hydroperoxides and conjugated dienes. However, plasma and liver MDA values did not change between diets.

The activity of the antioxidant enzymes SOD, CAT, GR and GPx, and the redox balance in terms of GSSG/GSH ratio were not different between dietary groups in both plasma and liver tissue. ORAC values also indicated no differences in the plasma and liver antioxidant capacity of rats fed control or HFHS diet.

3.2. Evaluation of protein oxidation in plasma

As evidenced in Fig. 2, long–term HFHS consumption triggered a significant increase of global protein carbonylation level in plasma. Fig. 2A shows total plasma proteins resolved on 1–D SDS–PAGE and stained with Coomassie blue. Fig. 2B shows plasma FTSC–labeled proteins resolved on 1–D gels. Graphical representation of global carbonylation indexes in plasma is included in Fig. 2C. Statistical analysis on individual protein bands revealed that the most abundant plasma protein was also the major protein target of oxidative damage accordingly to its highest carbonylation level (Fig. 2D). This protein was successfully identified as serum albumin by tandem mass spectrometry (P02770, Sequest HT score: 696.5), and constitutes approximately 55% of total plasma proteins [42]. In the HFHS group, albumin underwent an increase higher than 50% in carbonylation as compared to the control group, and that increment represented about 50% of the increase of total protein carbonylation in plasma from HFHS rats.

3.3. Evaluation of protein oxidation in skeletal muscle

Global protein carbonylation indexes were calculated for LIS and HIS fractions of skeletal muscle, and respectively compared between diets (data not shown). These indexes were not significantly different between dietary groups, and therefore, there was not a significant effect of the high caloric diet. However, some aspects of the carbonylated protein profiles should be highlighted (supplementary Figures S1 and S2). In the LIS muscular fraction, Coomassie–stained gels showed that proteins were mainly concentrated between ~45 and ~35 kDa (supplementary Figure S1A). However, the most carbonylated proteins were located at lower mass ranges (~40 and ~20 kDa) (Figure S1B). Thereby, we found high–concentrated, low–oxidized protein bands (as band 5) and low–concentrated, high–oxidized protein bands as band 9, and particularly band 10, for which carbonylation index was one order of magnitude higher to the rest of proteins (Figure S1C). Protein oxidation occurring in the HIS fraction appeared to be homogeneously distributed throughout mass and abundance protein ranges (supplementary Figures S2A and S2B), and their carbonylation indexes were in the same order of magnitude (Fig. S2C).

3.4. Evaluation of protein oxidation in liver

The analysis of 1–D gels of liver LIS and HIS proteins showed significant differences in the global protein carbonylation levels of control and HFHS groups (Fig. 3 and 4). Interestingly, LIS and HIS proteins were significantly more carbonylated in the HFHS rats than control animals ($p < 0.05$ and $p < 0.001$, respectively). Similarly to plasma, liver proteins exhibited different susceptibility to the oxidative damage induced by HFHS diet, and such specific vulnerability was found in LIS and HIS fractions (Figure 3, bands 1–6 and Figure 4, bands 1–2). Thus, some particular proteins seemed to be targets of the carbonylation triggered by HFHS diet consumption.

To deepen on the characterization of carbonylated proteins targeted by HFHS diets, 2–D gels were performed to isolate and identify individual proteins. Fig. 5A and Fig. 5B show respectively LIS and HIS fractions resolved on 2–D gels. Only proteins displaying a significant change in their protein carbonylation level were marked in gels.

Seven protein spots from LIS fraction displayed a significant change in carbonylation (Fig. 5A and Table 3). Six of them showed an increment of carbonylation in samples corresponding to HFHS diet (spots numbered as 1, 2, 3, 4, 5 and 6). Only one protein spot presented a reduced carbonylation level in the HFHS group (spot 7). Tandem mass spectrometry analysis revealed the following identifications: spot 1 was assigned to mitochondrial enzyme carbamoyl–phospate synthase (ammonia) (CPSase1), spot 2 was identified as albumin, spot 3 was, in fact, a mixture of two different proteins; one was bifunctional ATP–dependent dihydroxyacetone kinase/FAD–AMP lyase (cyclizing) and other was catalase. Spot 4 was other mitochondrial enzyme, aldehyde dehydrogenase (ALDH2). Argininosuccinate synthetase (ASS) was comprised in spot 5. Spot 6 contained regucalcin and finally, spot 7 was the mitochondrial aspartate transaminase (AST2).The analysis of 2–D HIS protein gels (Fig. 5B and Table 3) revealed four protein spots (numbered as 8, 9, 10 and 11) with increased carbonylation in rats fed a HFHS diet. Protein spot 8 was identified as the subunit beta of mitochondrial ATP synthase. Spot 9 was actin cytoplasmic 1. Two different proteins were mingled in spot 10: mitochondrial aldehyde dehydrogenase and 4–trimethylaminobutyraldehyde dehydrogenase. Finally, spot 11 was also a mitochondrial protein, glutamate dehydrogenase 1 (GDH1). Protein identifications and their cellular compartments are summarized in Table 3 and detailed in supplementary Tables S1 and S2. Two proteins were found in spot 3 and in spot 10. The efforts made using high–resolution IEF strips (18 cm) in order to resolve the two proteins resulted unsuccessful. Hence, it was impossible to know if the change in protein carbonylation was due to a single protein or both.

Further investigation was performed to identify oxidative sites and specific carbonyl modifications. Among the 13 proteins listed in Table 3, corresponding to the 11 spots of interest, all proteins except four of them (bifunctional ATP–dependent dihydroxyacetone kinase/FAD–AMP lyase, catalase, 4–trimethylaminobutyraldehyde dehydrogenase and ASS) demonstrated to have at least one oxidation site. Carbonylation sites found on each protein are shown in Table 3. It should be noted that all proteins exhibited proline residues oxidized (to glutamic semialdehyde and/or 5–oxoproline), with the exception of proteins found in spot 10. Moreover, ALDH2 (spot 4 and 10) and GDH1 (spot 11) showed carbonylation sites on tryptophan residues result of the oxidation of their side chain. Serine residues held carbonyl moieties arising from oxidation of the side chain as shown for serum albumin and ALDH2. Oxidation of arginine to glutamic semialdehyde was detected on two proteins, CPS1 and albumin. Finally, some oxidative modifications were detected on single carbonylated proteins: CPS1 showed carbonylation sites on threonine (from oxidation of its side chain), asparagine and cysteine residues (which were respectively bound to acetaldehyde and 2–hexenal); lysine residues bound to acrolein were found in AST2 and histidine residues were oxidized to 2–oxohistidine and forming a Schiff base adduct with acetaldehyde on cytoplasmic actin 1.

4. Discussion

The results presented here show that long–term consumption of a HFHS diet causes a characteristic carbonylation pattern in plasma and liver. Meanwhile proteins from skeletal muscle are similarly carbonylated in animals fed HFHS and control diets. This characteristic map is in agreement with a previous study describing an increment of liver protein oxidation in HFHS diet-fed rats, while protein oxidation in skeletal muscle was not modified [17].

The distinctive protein oxidation found in the HFHS group occured in parallel with a significant increase in abdominal and liver fat, body weight and insulin levels in plasma. Abdominal fat and insulin resistance are strongly related in humans [43] and insulin resistance plays also an important role in liver fat accumulation and inflammation [44]. Our results also indicate a higher lipid peroxidation in terms of hydroperoxides and conjugated dienes in livers from HFHS rats. It is in agreement to their elevated hepatic steatosis and inflammation, and previous correlations of an increased lipid peroxidation in animal models of NAFLD [45]. Thus, the increment of liver conjugated dienes and hidroperoxides found in the study can be related with hepatic steatosis and inflammation. The higher protein carbonylation and the increased production of primary and intermediary oxidation products did not correlate with the MDA values found in liver. Previous investigations had indicated that TBA reaction is not specific for the MDA generated by lipid peroxidation and that MDA analysis may have interferences in complex biological samples such as liver tissue [46, 47].

Regards to antioxidant activities in liver, they did not show any significant differences between rats. This could be a consequence of metabolic adaptations of the liver to a prolonged high caloric consumption as previously suggested [48].

Insulin resistance and protein carbonylation seem to be closely related, through activation of c-jun NH(2)-terminal kinases (JNK) by an increased protein carbonylation level [5, 19]. On the contrary, plasma glucose values did not change between diets. This normoglycemia was coherent with the absence of change in the glycated hemoglobin percentage observed [49]. These results highlight the higher insulin level required in the HFHS group to maintain normal glucose levels compared to rats fed control diet; this is in term the earliest sign of the onset of type-2 diabetes in HFHS rats [50].

Our results also showed that HFHS diet did not elevate plasma triglycerides and cholesterol levels. Similar plasma lipid profiles with different combinations of high caloric diets have been previously found [17, 51, 52], and even, several studies have reported decreased plasma triglycerides and cholesterol levels [53–56]. Since it is well recognized that high refined sugar dietary content (up 60% of calories) can elevate plasma triglycerides levels [2, 57], the level of sucrose in our diet was possibly low (27.2% of calories) to produce a hypertriglyceridemic state. Moreover, an increase in triglyceride clearance by the adipose tissue and liver, evidenced in this work through the increase of weight and the liver steatosis and inflammation, may also contribute to maintain, or even to decrease, plasma triglycerides levels [51]. The high level of fat in our diet could tend to inhibit fatty acid synthesis [55]. This fact together with the low level of cholesterol in the HFHS diet (0.05%, from milk fat), which was possibly not enough to elevate cholesterol levels in plasma, may explain that HFHS feeding did not change cholesterol levels that even seemed to tend to lower concentrations. Previous studies have reported inconsistent data for the induction of hypercholesterolemia in rats by a pure high fat diet without cholesterol added [58]. Successful dietary interventions aimed to achieve hypercholesterolemia currently incorporate high caloric diets with more than 0.2% cholesterol [17, 51, 56].

The map of the characteristic carbonylation pattern of proteins can provide a new insight into the pathogenesis of metabolic diseases derived from the high consumption of fat and refined carbohydrate. We found that plasma albumin is target of oxidative stress triggered by the intake of a HFHS diet rich in milk fat. Milk fat is composed mainly of triglycerides in which main fatty acids are palmitate, stearate, oleate, linoleate and linolenate [59]. In a previous work, we demonstrated that omega–3 fatty acids of marine origin (EPA and DHA), especially when given at 1:1 ratio, reduced plasma albumin oxidation, in comparison with ot**her fatty acids, mainly α–** linolenic acid from linseed oil and linoleic acid from soybean oil, in healthy rats [12]. It appears that the quantity and/or quality of dietary fat influences plasma albumin oxidation. Perhaps, the role of albumin as fatty acid transporter in plasma might explain this interdependence. The increased carbonylation of albumin, an important antioxidant in plasma [60], suggests that HFHS diet triggers oxidative stress and particularly oxidative damage on proteins. According with this, Pandey et al. [61] noted that type–2 diabetic patients showed higher plasma carbonyl levels and more advanced oxidation protein products than healthy people, and these protein modifications were postulated to be among the molecular mechanisms leading to diabetic complications.

Liver profiles revealed that mitochondrial proteins are the main targets of the differential diet–induced carbonylation, highlighting the importance of subcellular localizations of the proteins. Four central proteins associated to nitrogen metabolism suffered significant oxidative transformations. Mitochondrial carbamoyl–phosphate synthase (CPSase1) and argininosuccinate synthetase (ASS) (key enzymes from urea cycle) together with glutamate dehydrogenase 1 (GDH1) were more carbonylated in the HFHS group. Only mitochondrial aspartate transaminase (AST2) appeared less oxidized by HFHS diet. Such alterations can influence amino acid and protein metabolism. Consistent with this, Barber et al. [62] reported that the consumption of high **caloric diets, specifically "cafeteria" diet,** causes a decline in the activity of the enzymes of urea cycle. Interestingly, enzymatic activities of CPSase1 and ASS showed the most dramatic reduction. The level of CPSase1 also significantly decreased in a genetic rat model of obesity and type–2 diabetes [63]. A metabolomic study revealed that HFHS diet reduces plasma levels of nitrogenous compounds, including urea [64]. Moreover, cafeteria–fed rats also showed high circulating amino acids levels [65]. Accordingly, mitochondrial GDH1 plays a central role in the catabolism of amino acids, particularly, in the branched–chain amino acids (valine, leucine and isoleucine) catabolism [66]. The carbonylation observed for GDH1 in HFHS rats could contribute to explain the higher levels of amino acids in plasma, as well as the reduced urea production caused by this kind of diets.

Unlike the rest of the identified proteins, HFHS diet reduced the carbonylation level of the mitochondrial AST2, a multifunctional enzyme that plays a role in amino acid metabolism, and in urea and tricarboxylic acid cycles. Interestingly, AST2 was less oxidized in soybean oil fed–rats compared to fish oil fed–rats, just the opposite behavior to the other liver proteins which were more oxidized by soybean supplementation [12]. More investigation is needed to explain the impact of diet on AST2 carbonylation and the biological relevance of its differential behavior in terms of carbonylation.

Feillet–Coudray et al. [17] found lowered activities of the complex II and complexes II+III of the liver mitochondrial respiratory chain in HFHS–fed rats. Besides, our results suggest that ATP synthase (complex V) may lose activity due to its higher carbonylation in HFHS–fed rats. This fact could reduce oxidative phosphorylation and lower ATP cellular concentrations, to finally result in mitochondrial disruption [67]. Supporting this hypothesis, Guo et al [68] reported that the *in vitro* carbonylation of beta subunit of ATP synthase drastically decreases the enzyme activity. Moreover, lower ATP production due to reduction of oxidative phosphorylation could increase the accumulation of oxidized proteins by inhibiting the mitochondrial ATP–dependent proteases, specifically of the ATP–dependent Lon protease that is implicated in the removal of these oxidized proteins. [7, 69]. Taking into consideration that the reduced mitochondrial enzyme activity precedes the development of NAFLD and insulin resistance [70], the higher level of mitochondrial enzyme carbonylation observed was consistent with the hyperinsulinemia and fatty liver developed by HFHS-fed rats.

Presumably, the higher carbonylation level of mitochondrial aldehyde dehydrogenase 2 (ALDH2) and regucalcin in HFHS-fed rats may accelerate the oxidative deterioration of hepatic cells because both enzymes are linked to the cellular antioxidant defense. ALDH2 is involved in the antioxidant defense against toxic lipid peroxidation carbonyls as 4-hydroxy-2-nonenal [71] and enzymes belonging to the ALDH family are carbonylation targets in adipose tissue of obese and insulin resistant mice [6]. Regucalcin has an activating effect on superoxide dismutase (SOD) [72], and suppressive on nitric oxide (NO) synthase activity in liver cytosol [73]. Moreover, regucalcin appears to be a key molecule in lipid metabolic disorders and diabetes [74].

Finally, actin cytoplasmic 1 was significantly carbonylated in the HFHS group. Since actin is essential in the maintenance of cellular structure and functionality, its damage is associated with several diseases [75]. Thereby, HFHS-fed rats could potentially suffer filament disruption and functional losses.

The identification of the carbonylated sites on specific proteins strengthened the occurrence of oxidation in these proteins. At present, few carbonylation sites on proteins have been detected *in vivo* and the potential impact of a certain oxidized amino acid found on a protein is not sufficiently known [76]. In this study, we found oxidized residues of proline, histidine, serine, arginine, asparagine, threonine, lysine and tryptophan in specific proteins. More research is needed to understand the individual significance of these carbonylated residues.

Oxidative modifications can alter biological protein activity by increasing their propensity to cross–link and precipitation, causing difficulties in their degradation, and enhancing their cellular toxicity. The identification of the carbonylated sites on proteins can be a good starting point to explain how specific carbonylated proteins affect biological systems and to make the use of oxidized proteins as disease markers in the future more likely.

To sum up, HFHS diet causes a selective oxidative damage in proteins from different tissues. Results of this study indicate a different predisposition of plasma and liver proteins to suffer oxidative damage, being mitochondrial proteins the main targets of ROS attack. Some proteins, notably (albumin, CPSase1, ASS, GDH1, AST2, ALDH2, regucalcin, ATP synthase subunit beta, actin cytoplasmic 1) are the main targets of the ROS overproduced due to HFHS long–term consumption in the rat model. Given the huge importance and complexity of metabolic processes performed in the liver, this differential oxidative damage could contribute to explain how HFHS diets induce metabolic alterations leading to obesity, insulin resistance and NAFLD. Additionally, this protein carbonylation profile may be used in nutritional intervention studies as an early marker of diet induced metabolic disorders.

Acknowledgments

This investigation has been supported by the Spanish Ministry of Science and Innovation (Grants AGL2009–12374–C03–01, –02 and –03, IPT–2011–0828–90000). The Spanish Ministry of Science and Innovation is gratefully acknowledged for the doctoral fellowship to L. M. Xunta de Galicia and European Social Fund are also thankfully recognized by the financial support of the **postdoctoral "Isidro Parga Pondal" contract to M. P.** EMT gratefully thanks the Panamanian government for a SENACYT / IFARHU pre-doctoral fellowship. L.M. also thanks the USC (Spain) for its doctoral program. The authors thank Lorena Barros and María Jesús González for their excellent technical assistance and AFAMSA (Vigo, Spain) for the provision of raw material.

Abbreviations: 1-D, one-dimensional; 2-D, two-dimensional; 4-ONE, 4-oxo-2-nonenal; AIN, American Institute of Nutrition; ALDH2, aldehyde dehydrogenase 2; ASS, argininosuccinate synthetase; AST2, aspartate transaminase 2; CPSase 1, carbamoyl-phosphate synthase 1; GDH1, glutamate dehydrogenase 1; DNPH, 2,4-dinitrophenylhydrazine; DTT, dithiothreitol; EDTA, ethylenediaminetetracetic acid; FTSC, fluorescein-5-thiosemicarbazide; HNE, 4-hydroxy-2-nonenal; HPLC-FL, high-performance liquid chromatography-fluorescence; LC-ESI-IT-MS/MS, high-performance liquid chromatography coupled with electrospray ionization ion trap tandem mass spectrometry; MDA, malondialdehyde; NAFLD, nonalcoholic fatty liver disease; ROS, reactive oxygen species; SDS-PAGE, sodium dodecyl sulfate-polyacrylamide gel electrophoresis

References

[1] Dalle–Donne I, Giustarini D, Colombo R, Rossi R, Milzani A. Protein carbonylation in human diseases. Trends Mol Med. 2003;9:169–76.

[2] Panchal SK, Brown L. Rodent models for metabolic syndrome research. J Biomed Biotechnol. 2011;2011:351982.

[3] Brownlee M. Biochemistry and molecular cell biology of diabetic complications. Nature. 2001;414:813–20.

[4] Maddux BA, See W, Lawrence JC, Goldfine AL, Goldfine ID, Evans JL. Protection against oxidative stress–induced insulin resistance in rat L6 muscle cells by micromolar concentrations of α–lipoic acid. Diabetes. 2001;50:404–10.

[5] Ruskovska T, Bernlohr DA. Oxidative stress and protein carbonylation in adipose tissue – implications for insulin resistance and diabetes mellitus. J Proteomics. 2013;92:323–34.

[6] Grimsrud PA, Picklo MJ, Sr., Griffin TJ, Bernlohr DA. Carbonylation of adipose proteins in obesity and insulin resistance: identification of adipocyte fatty acid–binding protein as a cellular target of 4–hydroxynonenal. Mol Cell Proteomics. 2007;6:624–37.

[7] Bulteau AL, Szweda LI, Friguet B. Mitochondrial protein oxidation and degradation in response to oxidative stress and aging. Exp Gerontol. 2006;41:653–7.

[8] Stadtman ER, Levine RL. Protein oxidation. Ann N Y Acad Sci. 2000;899:191–208.

[9] Davies MJ, Dean R. Radical–mediated protein oxidation: from chemistry to medicine. Oxford: Oxford Science Publications. 1997.

[10] Choi J, Malakowsky CA, Talent JM, Conrad CC, Gracy RW. Identification of oxidized plasma proteins in Alzheimer's disease. Biochem Biophys Res Commun. 2002;293:1566–70.

[11] Himmelfarb J, McMonagle E. Albumin is the major plasma protein target of oxidant stress in uremia. Kidney Int. 2001;60:358–63.

[12] Méndez L, Pazos M, Gallardo JM, Torres JL, Pérez-Jiménez J, Nogués R, et al. Reduced protein oxidation in Wistar rats supplemented with marine omega-3 PUFAs. Free Radic Biol Med. 2013;55:8–20.

[13] Alisi A, Bruscalupi G, Pastore A, Petrini S, Panera N, Massimi M, et al. Redox homeostasis and posttranslational modifications/activity of phosphatase and tensin homolog in hepatocytes from rats with diet-induced hepatosteatosis. J Nutr Biochem. 2012;23:169–78.

[14] Morrison CD, Pistell PJ, Ingram DK, Johnson WD, Liu Y, Fernandez-Kim SO, et al. High fat diet increases hippocampal oxidative stress and cognitive impairment in aged mice: implications for decreased Nrf2 signaling. J Neurochem. 2010;114:1581–9.

[15] Dandona P, Mohanty P, Ghanim H, Aljada A, Browne R, Hamouda W, et al. The suppressive effect of dietary restriction and weight loss in the obese on the generation of reactive oxygen species by leukocytes, lipid peroxidation, and protein carbonylation. J Clin Endocrinol Metab. 2001;86:355–62.

[16] Matsuzawa-Nagata N, Takamura T, Ando H, Nakamura S, Kurita S, Misu H, et al. Increased oxidative stress precedes the onset of high-fat diet-induced insulin resistance and obesity. Metabolism. 2008;57:1071–7.

[17] Feillet-Coudray C, Sutra T, Fouret G, Ramos J, Wrutniak-Cabello C, Cabello G, et al. Oxidative stress in rats fed a high-fat high-sucrose diet and preventive effect of polyphenols: Involvement of mitochondrial and NAD(P)H oxidase systems. Free Radic Biol Med. 2009;46:624–32.

[18] Frohnert BI, Sinaiko AR, Serrot FJ, Foncea RE, Moran A, Ikramuddin S, et al. Increased adipose protein carbonylation in human obesity. Obesity. 2011;19:1735–41.

[19] Yuzefovych LV, Musiyenko SI, Wilson GL, Rachek LI. Mitochondrial DNA damage and dysfunction, and oxidative stress are associated with endoplasmic reticulum stress, protein degradation and apoptosis in high fat diet–induced insulin resistance mice. PLoS One. 2013;8:e54059.

[20] Bucolo G, David H. Quantitative determination of serum triglycerides by the use of enzymes. Clin Chem. 1973;19:476–82.

[21] Young DS, Friedman RB. Effects of disease on clinical laboratory tests. Washington, DC: AACC Press. 2001.

[22] Sharp P, Rainbow S. Continuous glucose monitoring and haemoglobin A(1c). Ann Clin Biochem. 2002;39:516–7.

[23] Bligh EG, Dyer WJ. A rapid method of total lipid extraction and purification. Can J Biochem Physiol. 1959;37:911–7.

[24] Herbes SE, Allen CP. Lipid quantification of freshwater invertebrates: method modification for microquantitation. Can J Fish Aquat Sci. 1983;40:1315–7.

[25] AOCS. Official and tentative methods of the American Oil Chemists' Society. 4th ed. Champain, IL: D Firestone. AOCS.; 1989.

[26] Chapman RA, Mackay K. The estimation of peroxides in fats and oils by the ferric thiocyanate method. J Am Oil Chem Soc. 1949;26:360–3.

[27] Mendes R, Cardoso C, Pestana C. Measurement of malondialdehyde in fish: A comparison study between HPLC methods and the traditional spectrophotometric test. Food Chem. 2009;112:1038–45.

[28] Mateos R, Lecumberri E, Ramos S, Goya L, Bravo L. Determination of malondialdehyde (MDA) by high–performance liquid chromatography in serum and liver as a biomarker for oxidative stress: Application to a rat model for hypercholesterolemia and evaluation of the effect of diets rich in phenolic antioxidants from fruits. J Chromatogr B. 2005;827:76–82.

[29] Fukunaga K, Suzuki T, Takama K. Highly sensitive high–performance liquid chromatography for the measurement of malondialdehyde in biological samples. J Chromatogr. 1993;621:77–81.

[30] Misra HP, Fridovich I. The role of superoxide anion in the autoxidation of epinephrine and a simple assay for superoxide dismutase. J Biol Chem. 1972;247:3170–5.

[31] Cohen G, Dembiec D, Marcus J. Measurement of catalase activity in tissue extracts. Anal Biochem. 1970;34:30–8.

[32] Wheeler CR, Salzman JA, Elsayed NM, Omaye ST, Korte DW, Jr. Automated assays for superoxide dismutase, catalase, glutathione peroxidase, and glutathione reductase activity. Anal Biochem. 1990;184:193–9.

[33] Hissin PJ, Hilf R. A fluorometric method for determination of oxidized and reduced glutathione in tissues. Anal Biochem. 1976;74:214–26.

[34] Ou B, Hampsch–Woodill M, Prior RL. Development and validation of an improved oxygen radical absorbance capacity assay using fluorescein as the fluorescent probe. J Agric Food Chem. 2001;49:4619–26.

[35] Taltavull N, Munoz–Cortes M, Lluis L, Jove M, Fortuno A, Molinar–Toribio E, et al. Eicosapentaenoic acid/docosahexaenoic acid 1:1 ratio improves histological alterations in obese rats with metabolic syndrome. Lipids Health Dis. 2014;13:31.

[36] Smith PK, Krohn RI, Hermanson GT, Mallia AK, Gartner FH, Provenzano MD, et al. Measurement of protein using bicinchoninic acid. Anal Biochem. 1985;150:76–85.

[37] Chaudhuri AR, de Waal EM, Pierce A, Van Remmen H, Ward WF, Richardson A. Detection of protein carbonyls in aging liver tissue: A fluorescence–based proteomic approach. Mech Ageing Dev. 2006;127:849–61.

[38] Pazos M, da Rocha AP, Roepstorff P, Rogowska–Wrzesinska A. Fish proteins as targets of ferrous–catalyzed oxidation: Identification of protein carbonyls by fluorescent labeling on two–dimensional gels and MALDI–TOF/TOF mass spectrometry. J Agricult Food Chem. 2011;59:7962–77.

[39] Bradford MM. A rapid and sensitive method for the quantitation of microgram quantities of protein utilizing the principle of protein–dye binding. Anal Biochem. 1976;72:248–54.

[40] Laemmli UK. Cleavage of structural proteins during the assembly of the head of bacteriophage T4. Nature. 1970;227:680–5.

[41] Jensen ON, Wilm M, Shevchenko A, Mann M. Sample preparation methods for mass spectrometric peptide mapping directly from 2–DE gels. In: Link AJ, editor. 2–D Proteome Analysis Protocols. Totowa, NJ: Humana Press; 1998. p. 513–30.

[42] Anderson NL, Anderson NG. The human plasma proteome: history, character, and diagnostic prospects. Mol Cell Proteomics. 2002;1:845–67.

[43] Carey DG, Jenkins AB, Campbell LV, Freund J, Chisholm DJ. Abdominal fat and insulin resistance in normal and overweight women: Direct measurements reveal a strong relationship in subjects at both low and high risk of NIDDM. Diabetes. 1996;45:633–8.

[44] Matteoni CA, Younossi ZM, Gramlich T, Boparai N, Liu YC, McCullough AJ. Nonalcoholic fatty liver disease: a spectrum of clinical and pathological severity. Gastroenterology. 1999;116:1413–9.

[45] Lieber CS, Leo MA, Mak KM, Xu Y, Cao Q, Ren C, et al. Model of nonalcoholic steatohepatitis. Am J Clin Nutr. 2004;79:502–9.

[46] Devasagayam TP, Boloor KK, Ramasarma T. Methods for estimating lipid peroxidation: an analysis of merits and demerits. Indian J Biochem Bio. 2003;40:300–8.

[47] Janero DR. Malondialdehyde and thiobarbituric acid–reactivity as diagnostic indices of lipid peroxidation and peroxidative tissue injury. Free Radic Biol Med. 1990;9:515–40.

[48] Kučera O, Garnol T, Lotková H, Staňnkováa P, Mazurová Y, Hroch M, et al. The effect of rat strain, diet composition and feeding period on the development of a nutritional model of non–alcoholic fatty liver disease in rats. Physiol Res. 2011;60:317–28.

[49] Sikaris K. The correlation of hemoglobin A1c to blood glucose. J Diabetes Sci Technol. 2009;3:429–38.

[50] Weir GC, Bonner–Weir S. Five stages of evolving beta–cell dysfunction during progression to diabetes. Diabetes. 2004;53:S16–S21.

[51] Yang Z–H, Miyahara H, Takeo J, Katayama M. Diet high in fat and sucrose induces rapid onset of obesity–related metabolic syndrome partly through rapid response of genes involved in lipogenesis, insulin signalling and inflammation in mice. Diabetol Metab Syndr. 2012;4:32.

[52] Boqué N, Campión J, Paternain L, García–Díaz DF, Galarraga M, Portillo MP, et al. Influence of dietary macronutrient composition on adiposity and cellularity of different fat depots in Wistar rats. J Physiol Biochem. 2009;65:387–95.

[53] Chalkley SM, Hettiarachchi M, Chisholm DJ, Kraegen EW. Long–term high–fat feeding leads to severe insulin resistance but not diabetes in Wistar rats. Am J Physiol Endocrinol Metab. 2002;282:E1231–8.

[54] Lomba A, Milagro FI, García–Díaz DF, Marti A, Campión J, Martínez JA. Obesity induced by a pair–fed high fat sucrose diet: methylation and expression pattern of genes related to energy homeostasis. Lipids Health Dis. 2010;9:60.

[55] Hallfrisch J, Cohen L, Reiser S. Effects of feeding rats sucrose in a high fat diet. J Nutr. 1981;111:531–6.

[56] Yamamoto Y, Oue E. Antihypertensive effect of quercetin in rats fed with a high–fat high–sucrose diet. Biosci Biotechnol Biochem. 2006;70:933–9.

[57] Angelova P, Boyadjiev N. A review on the models of obesity and metabolic syndrome in rats. TJS. 2013;1:5–12.

[58] Buettner R, Schölmerich J, Bollheimer LC. High–fat diets: modeling the metabolic disorders of human obesity in rodents. Obesity. 2007;15:798–808.

[59] Jensen RG, Ferris AM, Lammi–Keefe CJ. The composition of milk fat. J Dairy Sci. 1991;74:3228–43.

[60] Halliwell B. Albumin–An important extracellular antioxidant? Biochem Pharmacol. 1988;37:569–71.

[61] Pandey KB, Mishra N, Rizvi SI. Protein oxidation biomarkers in plasma of type 2 diabetic patients. Clin Biochem. 2010;43:508–11.

[62] Barber T, Vina JR, Vina J, Cabo J. Decreased urea synthesis in cafeteria–diet–induced obesity in the rat. Biochem J. 1985;230:675–81.

[63] Rector RS, Thyfault JP, Uptergrove GM, Morris EM, Naples SP, Borengasser SJ, et al. Mitochondrial dysfunction precedes insulin resistance and hepatic steatosis and contributes to the natural history of non-alcoholic fatty liver disease in an obese rodent model. J Hepatol. 2010;52:727–36.

[64] Etxeberria U, de la Garza AL, Martínez JA, Milagro FI. Diet-induced hyperinsulinemia differentially affects glucose and protein metabolism: a high-throughput metabolomic approach in rats. J Physiol Biochem. 2013;69:613–23.

[65] Rafecas I, Esteve M, Fernández-López JA, Remesar X, Alemany M. Individual amino acid balances in young lean and obese Zucker rats fed a cafeteria diet. Mol Cell Biochem. 1993;121:45–58.

[66] Islam MM, Nautiyal M, Wynn RM, Mobley JA, Chuang DT, Hutson SM. Branched-chain amino acid metabolon: interaction of glutamate dehydrogenase with the mitochondrial branched-chain aminotransferase (BCATm). J Biol Chem. 2010;285:265–76.

[67] Pieczenik SR, Neustadt J. Mitochondrial dysfunction and molecular pathways of disease. Exp Mol Pathol. 2007;83:84–92.

[68] Guo J, Prokai-Tatrai K, Nguyen V, Rauniyar N, Ughy B, Prokai L. Protein targets for carbonylation by 4-hydroxy-2-nonenal in rat liver mitochondria. J Proteomics. 2011;74:2370–9.

[69] Bota DA, Ngo JK, Davies KJ. Downregulation of the human Lon protease impairs mitochondrial structure and function and causes cell death. Free Radic Biol Med. 2005;38:665–77.

[70] Erjavec N, Bayot A, Gareil M, Camougrand N, Nystrom T, Friguet B, et al. Deletion of the mitochondrial Pim1/Lon protease in yeast results in accelerated aging and impairment of the proteasome. Free Radic Biol Med. 2013;56:9–16.

[71] Yoon M, Madden MC, Barton HA. Developmental expression of aldehyde dehydrogenase in rat: a comparison of liver and lung development. Toxicol Sci. 2006;89:386–98.

[72] Fukaya Y, Yamaguchi M. Regucalcin increases superoxide dismutase activity in rat liver cytosol. Biol Pharm Bull. 2004;27:1444–6.

[73] Yamaguchi M, Takahashi H, Tsurusaki Y. Suppressive role of endogenous regucalcin in the enhancement of nitric oxide synthase activity in liver cytosol of normal and regucalcin transgenic rats. J Cell Biochem. 2003;88:1226–34.

[74] Yamaguchi M, Murata T. Involvement of regucalcin in lipid metabolism and diabetes. Metabolism. 2013;62:1045–51.

[75] Dalle-Donne I, Rossi R, Giustarini D, Gagliano N, Lusini L, Milzani A, et al. Actin carbonylation: from a simple marker of protein oxidation to relevant signs of severe functional impairment. Free Radic Biol Med. 2001;31:1075–83.

[76] Madian AG, Regnier FE. Proteomic identification of carbonylated proteins and their oxidation sites. J Proteome Res. 2010;9:3766–80.

Figure Captions

Figure 1. Liver histology after haematoxylin/eosin staining of liver sections from a representative rat fed a A). CONTROL diet (200×) and B). HFHS diet (200×). Lobular inflammation cell infiltrations are marked up with a black arrow and steatosis is marked up, in part, with white arrows. Panels C) and D) show respectively the grade of steatosis and lobular inflammation found in CONTROL and HFHS rats, both expressed as percentages.

Figure 2. Effect of HFHS diet on carbonylation level of plasma proteins from male Sprague–Dawley rats. A). 1–DE Coomassie–stained gel of fresh plasma proteins from CONTROL and HFHS dietary groups. Lanes 1, 2, 3, 4, 5: CONTROL diet. Lane 6, 7, 8, 9, 10: HFHS diet. B). 1–DE FTSC–stained gel of fresh plasma proteins from CONTROL and HFHS dietary groups. Lanes 1, 2, 3, 4, 5: CONTROL diet. Lane 6, 7, 8, 9, 10: HFHS diet. C). Global plasma protein carbonylation index for CONTROL and HFHS dietary groups. Data are presented as mean ± SD. D). Plasma albumin carbonylation index for CONTROL and HFHS dietary groups. Data are presented as mean ± SD. *$p < 0.05$, **$p < 0.01$.

Figure 3. Effect of HFHS diet on carbonylation level of LIS liver proteins from male Sprague–Dawley rats. A). 1–DE Coomassie–stained gel of LIS proteins from CONTROL and HFHS dietary groups. Lanes 1, 2, 3, 4, 5: CONTROL diet. Lane 6, 7, 8, 9, 10: HFHS diet. B).1–DE FTSC–stained gel of LIS proteins from CONTROL and HFHS dietary groups. Lanes 1, 2, 3, 4, 5: CONTROL diet. Lane 6, 7, 8, 9, 10: HFHS diet. C). Global LIS protein carbonylation index for CONTROL and HFHS dietary groups. Marked bands (b1 to b6) showed differential protein carbonylation index. Data are presented as mean ± SD. *$p < 0.05$.

Figure 4. Effect of HFHS diet on carbonylation level of HIS liver proteins from male Sprague–Dawley rats. A). 1–DE Coomassie–stained gel of HIS proteins from CONTROL and HFHS

dietary groups. Lanes 1, 2, 3, 4, 5: CONTROL diet. Lane 6, 7, 8, 9, 10: HFHS diet. B).1–DE FTSC–stained gel of HIS proteins from CONTROL and HFHS dietary groups. Lanes 1, 2, 3, 4, 5: CONTROL diet. Lane 6, 7, 8, 9, 10: HFHS diet. C). Global HIS protein carbonylation index for CONTROL and HFHS dietary groups. Marked bands (b1 and b2) showed differencial protein carbonylation index. Data are presented as mean ± SD. *$p < 0.05$.

Figure 5. Representative 2–D gels for CONTROL and HFHS groups showing total and carbonylated protein profiles of LIS and HIS liver fractions. Coomassie–stained 2–D gels that represent the abundance of LIS liver proteins in CONTROL and HFHS diets are shown respectively in panels a) and c). The level of carbonylation of LIS liver proteins in CONTROL and HFHS diets by visualizing images of the FTSC–stained 2–D gels are shown respectively in panels b) and d). The corresponding Coomassie–stained 2–D gels of HIS liver proteins from CONTROL and HFHS rats are shown respectively in panels e) and g). FTSC–stained 2–D gels of HIS liver proteins from CONTROL and HFHS rats are shown respectively in panels f) and h). * indicate proteins with higher carbonylation index (FTSC intensity normalized by the Coomassie intensity) in HFHS rats at $p < 0.05$. § indicate proteins with lower carbonylation index in HFHS rats at $p < 0.05$. Numbered protein spots represent carbonylated proteins confidently identified, and they are listed in Table 3.

Table(s)

Table 1. Body measurements and metabolic variables in rats.

		Control (n=5)	HFHS (n=5)
Final body weight (g)		722.4 (95.6)	918.2 (93.3)*
Food intake (g/day)		26.7 (1.2)	21.9 (0.5)*
Energy intake (kcal/day)		77.4 (8.8)	101.0 (8.4)*
Total abdominal fat weight (g)		32.4 (13.8)	60.7 (9.3)**
Adiposity index (%)†		4.4 (1.2)	6.7 (1.5)*
Liver weight (g)		15.6 (3.6)	24.8 (6.8)*
Total liver lipids (mg/g)		2.3 (0.2)	8.8 (1.9)**
Hepatosomatic index (%)‡		2.1 (0.3)	2.7 (0.8)
Total cholesterol (mmol/L)		2.87 (0.40)	2.26 (0.20)
LDL-C (mmol/L)		0.42 (0.11)	0.29 (0.04)
HDL-C (mmol/L)		0.73 (0.06)	0.60 (0.06)
Triglycerides (mmol/L)		2.13 (0.34)	1.71 (0.33)
HbA1c (%)		5.7 (0.4)	5.0 (0.1)
Plasma glucose (mmol/L)		4.1 (0.4)	4.5 (0.5)
Plasma insulin (pmol/L)	Week 5	0.25 (0.10)	1.16 (0.11)**
	Week 9	0.27 (0.12)	0.80 (0.03)**
	Week 13	0.29 (0.14)	0.88 (0.05)**

†Adiposity index: (total abdominal fat × 100)/body weight.

‡Hepatosomatic index: (liver weight × 100)/body weight.

Results are means (standard deviation); n, number of rats. *$p<0.05$, **$p<0.01$ vs. CONTROL group

Table 2. Blood and liver oxidative stress parameters.

	Plasma		Liver	
	Control (n=5)	HFHS (n=5)	Control (n=5)	HFHS (n=5)
Conjugated dienes (nmol/mg protein)			10.2 (0.9)	87.8 (30.3)**
Lipid hydroperoxides (meqO2/kg protein)			2.3 (0.3)	4.2 (0.6)**
MDA (nmol/mg protein)	0.2 (0.05)	0.2 (0.05)	0.5 (0.1)	0.6 (0.1)
SOD (U/g Hb or g tissue)	2112.2 (644.9)	2576.0 (1417.9)	13.6 (6.8)	14.5 (5.0)
CAT (mmol/(min·g Hb or g T))	116.2 (9.2)	119.3 (7.7)	10.3 (3.6)	11.1 (3.4)
GR (U/g Hb or g T)	0.4 (0.2)	0.2 (0.1)	8.8 (1.1)	7.4 (3.2)
GPx (U/g Hb or g T)	107.4 (9.9)	112.2 (10.6)	35.8 (4.1)	43.9 (17.5)
ORAC (mmol TE/L P or kg T)	10.3 (0.6)	8.6 (2.0)	18.6 (1.0)	15.4 (3.1)
GSSG/GSH			2.6 (0.3)	2.5 (0.7)

Results are means (standard deviation); n, number of rats. *$p<0.05$, **$p<0.01$ vs. CONTROL group

Abbreviations: MDA, malondialdehyde; SOD, superoxide dismutase; CAT, catalase; GR, glutathione reductase; Gpx, glutathione peroxidase; GSSG/GSH, oxidized and reduced glutathione balance; Hb: hemoglobin; P, plasma; T, tissue; TE, Trolox–equivalents; Trolox, 6–hydroxy–2,5,7,8–tetramethylchroman–2–carboxylic acid

Table 3. Identification of LIS and HIS liver proteins with different carbonylation levels between dietary groups. Spots of interest were identified by LC–ESI–IT–MS/MS as described in the section 2.10. Protein spot nº refer to the numbered spots in 2–D gels shown in Fig. 5. For each protein spot, different parameters are indicated: tissue liver fraction, cellular component, significant peptides (FDR < 1%), % sequence coverage, protein carbonylation indexes and oxidative modifications found in each protein.

Spot Nº	LIS/HIS fraction	Identification	Accession	Celullar component	Significant Peptides (FDR < 1%)	Sequence Coverage (%)	Protein Carbonylation Index[b)] CONTROL (n=5)	Protein Carbonylation Index[b)] HFHS (n=5)	Oxidative modifications [b)]
1	LIS	Carbamoyl–phosphate synthase [ammonia], mitochondrial	P07756	Mitochondrion	44	46.53	0.55(0.21)	1.14(0.44)*	[1]N649,[1]N652 [4]C648 [5]T295, [5]T300 [6]P99,[6]P464,[6]P501, [6]P601 [7]R1039
2	LIS	Serum albumin	P02770	Cytoplasm	13	30.92	0.89(0.42)	1.85(0.82)*	[6]P510 [7]R509 [8]S513
3	LIS	Bifunctional ATP–dependent dihydroxyacetone kinase/FAD–AMP lyase (cyclizing)	Q4KLZ6	Cytoplasm	5	9.86	1.38(0.86)	3.33(1.27)*	
		Catalase	P04762	Peroxisome	2	5.69			
4	LIS	Aldehyde dehydrogenase, mitochondrial	P11884	Mitochondrion	16	41.04	2.55(1.11)	9.43(6.51)*	[6]P94 [8]S93 [10]W95 [11]P94
5	LIS	Argininosuccinate synthetase	P09034	Cytoplasm Outer mitochondrial membrane	5	13.59	0.41(0.13)	0.74(0.27)*	
6	LIS	Regucalcin	Q03336	Cytoplasm	5	24.75	0.31(0.26)	1.15(0.74)*	[6]P124
7	LIS	Aspartate transaminase, mitochondrial	P00507	Mitochondrion	10	32.33	1.57(0.52)	0.64(0.22)*	[2]K107 [6]P98 [11]P98
8	HIS	ATP synthase beta subunit	G3V6D3	Mitochondrion	23	69.19	0.83(0.16)	1.48(0.42)*	[11]P131,[11]P333,[11]P396,[11]P400, [11]P503,[11]P512

9	HIS	Actin, cytoplasmic 1	P60711	Cytoplasm	8	42.93	0.84(0.17)	1.37(0.26)*	^{1}H275 ^{3}H73 ^{11}P70
10	HIS	Aldehyde dehydrogenase, mitochondrial	P11884	Mitochondrion	15	49.,71	0.50(0.22)	1.14(0.31)*	^{9}W471
		4–trimethylaminobutyraldehyde dehydrogenase	Q9JLJ3	Cytoplasm	3	7.89			
11	HIS	Glutamate dehydrogenase 1, mitochondrial	P10860	Mitochondrion	16	42.11	0.45(0.08)	0.62(0.08)*	^{6}P224,^{6}P340 ^{9}W338 ^{10}W338

a) Protein Carbonylation Index :(FTSC/Coomassie Intensities). Results are means (standard deviation);n, number of rats. *$p<0.05$ vs. CONTROL group
b) 1 – Schiff base adduct with Acetaldehyde ; 2 – Michael–type adduct with Acrolein ; 3 – 2–Oxohistidine ; 4 – Michael–type adduct with 2–Hexenal ; 5 – 2–Amino–3–Ketobutiric ;6 – Glutamic semialdehyde (P), 7 – Glutamic semialdehyde (R) ; 8 – 3–Oxoalanine (S) ; 9 – Kynurenine ; 10 – N–formylkynurenine ; 11 – 5–Oxoproline

Figure(s)
Click here to download high resolution image

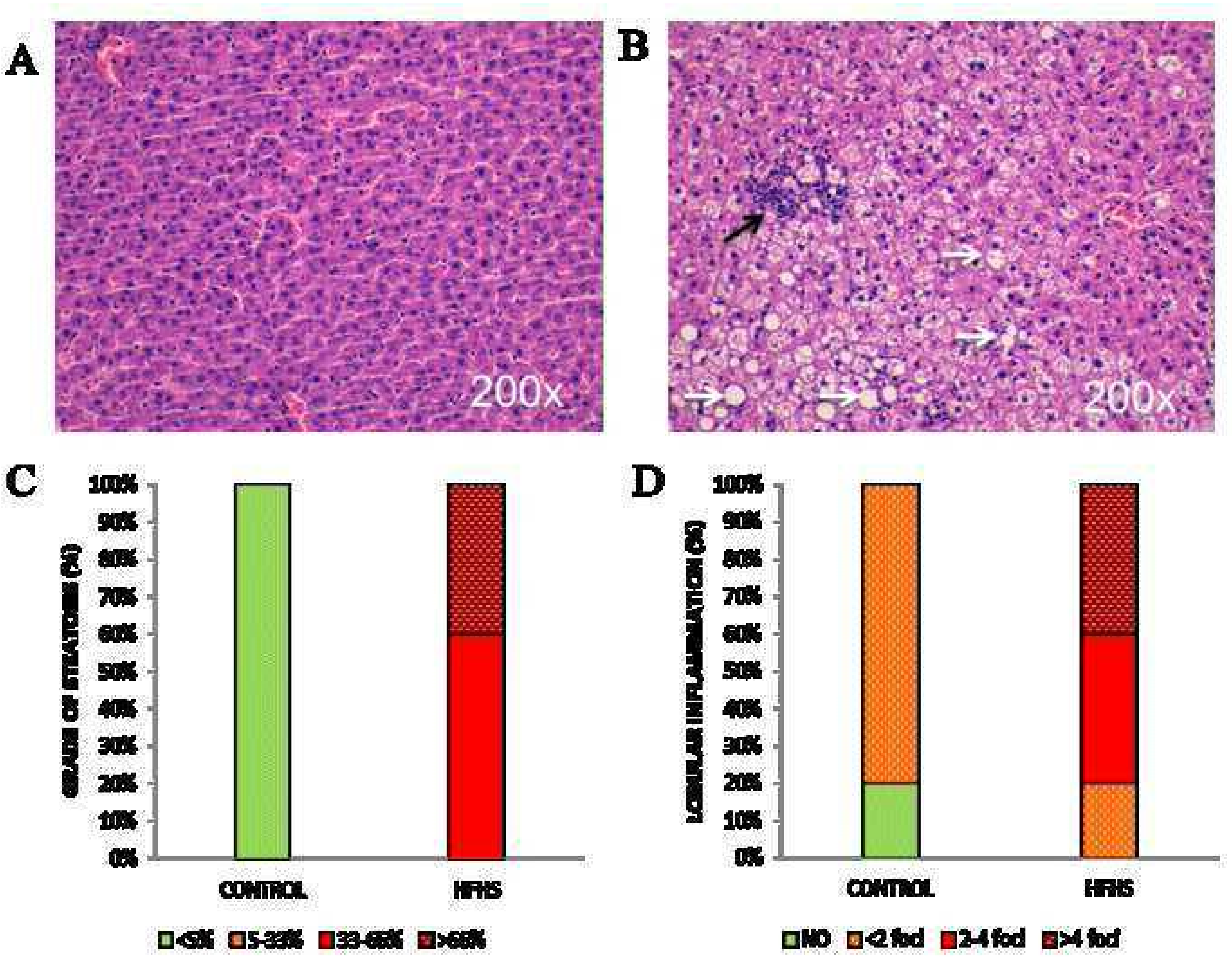

Figure(s)
Click here to download high resolution image

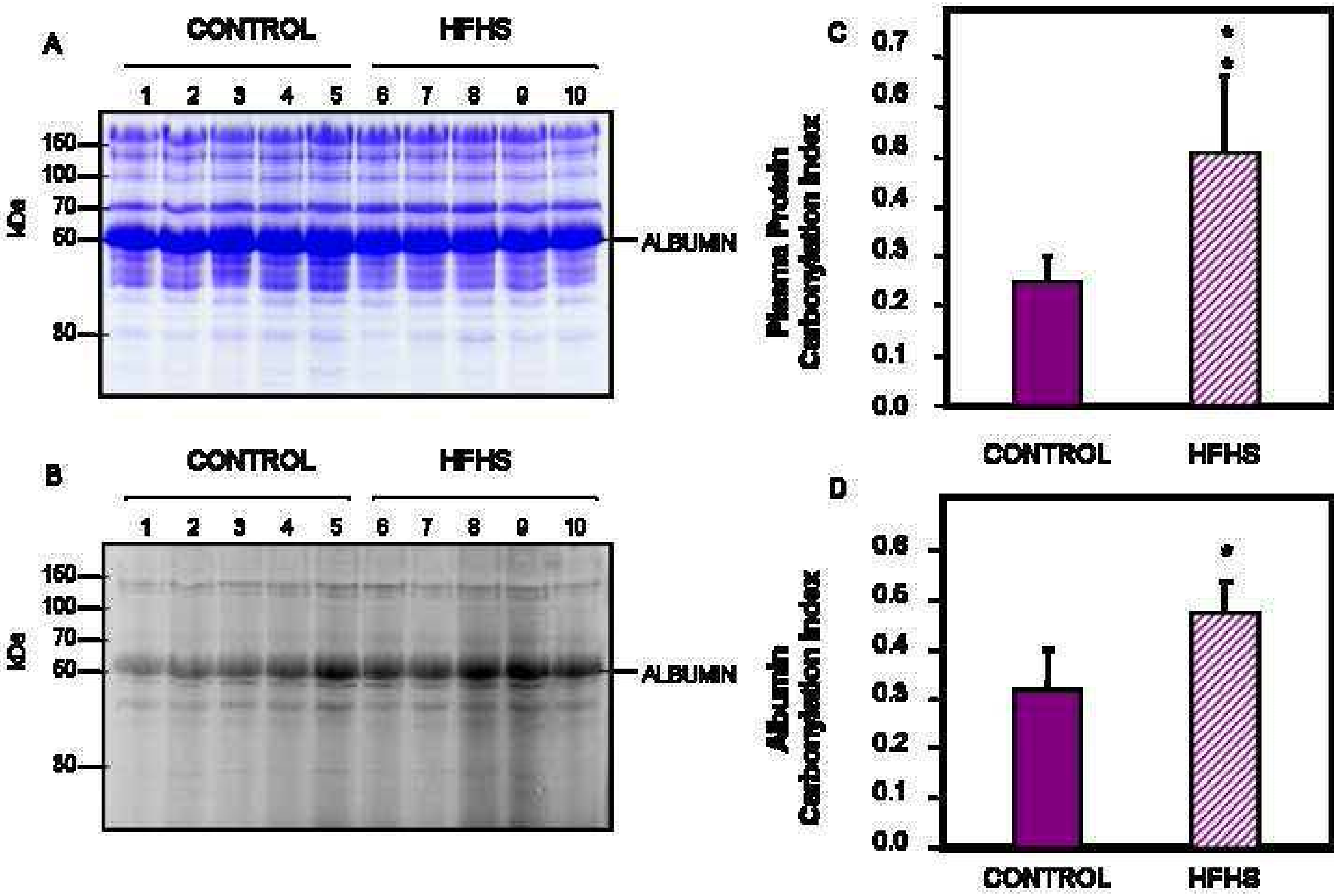

Figure(s)
Click here to download high resolution image

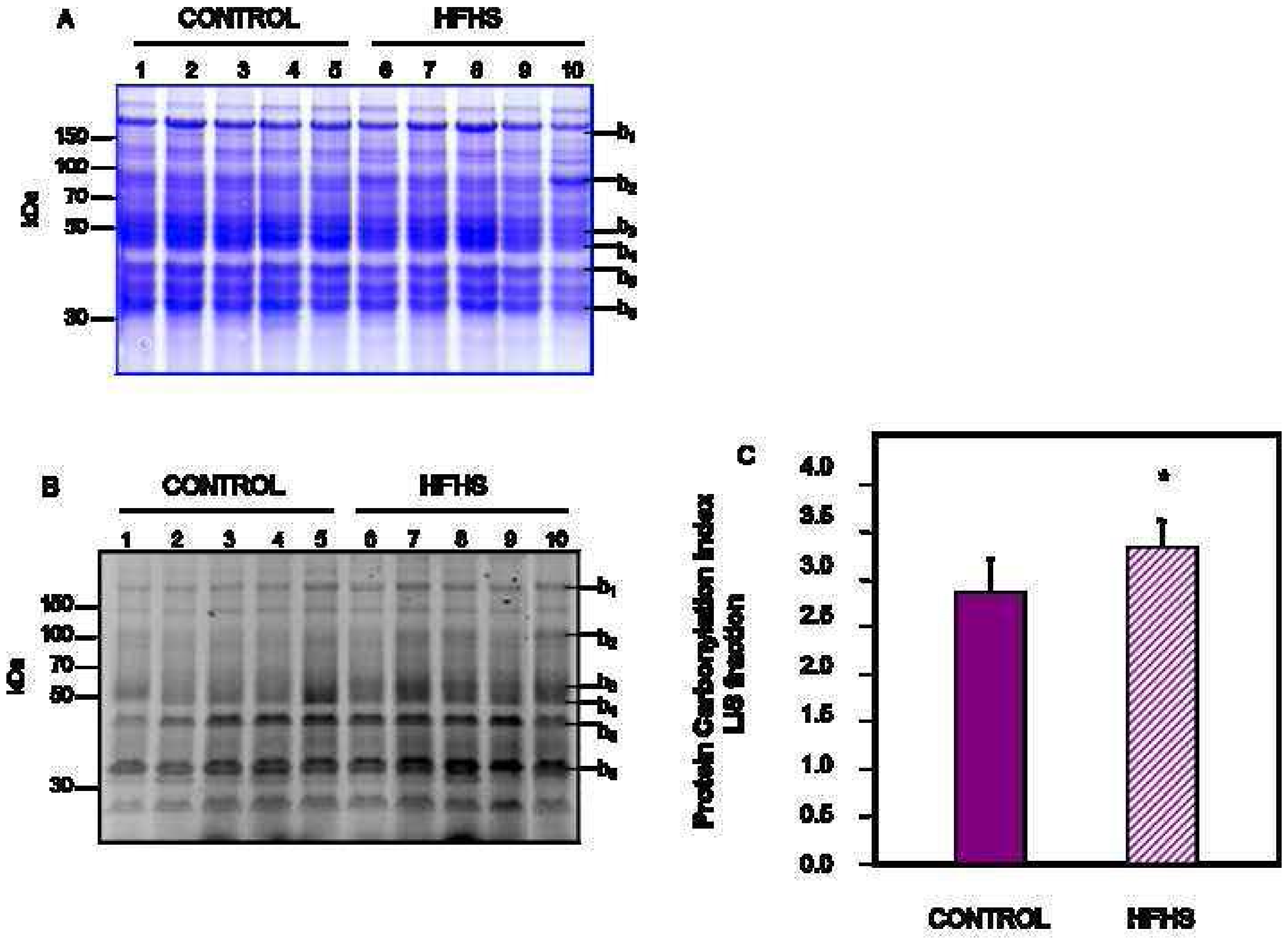

Figure(s)
Click here to download high resolution image

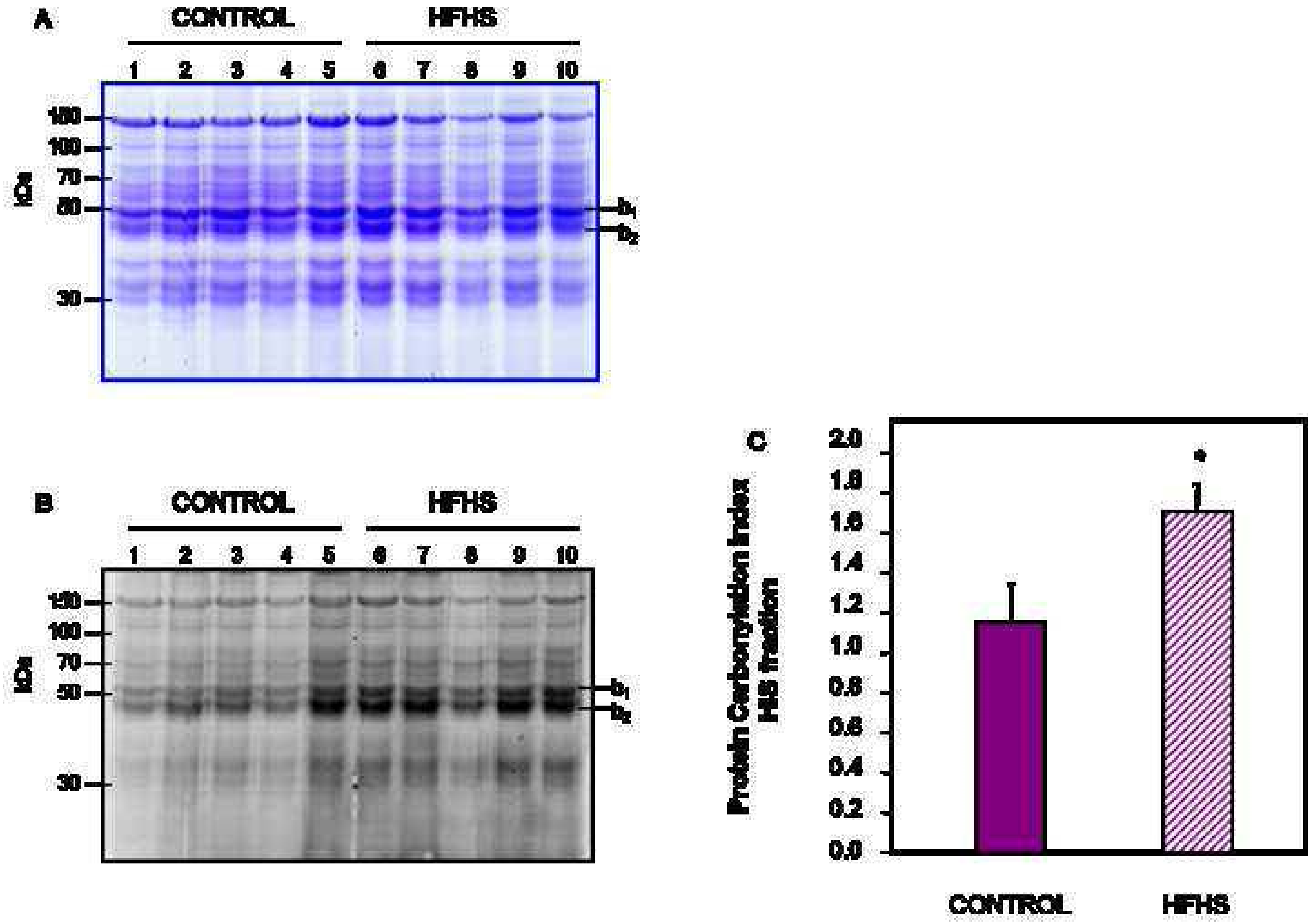

Figure(s)

Click here to download high resolution image

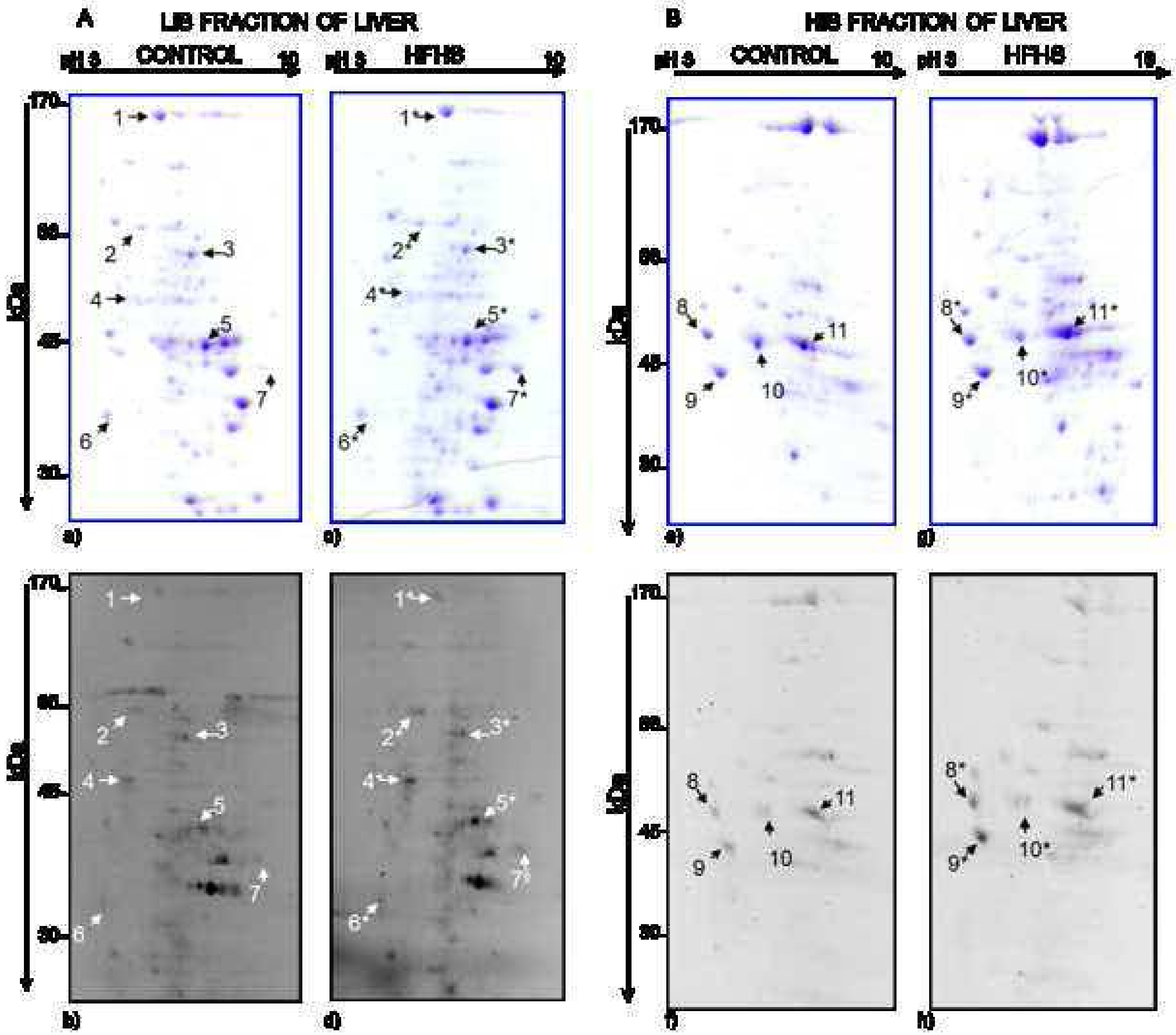

Supplemental file for online publication

Click here to download Supplemental file for online publication: SupplementaryTablesS1S2.xlsx